Stress-Regulated Translational Attenuation Adapts Mitochondrial Protein Import Through Tim17A Degradation

T. Kelly Rainbolt[1], **Neli Atanassova**[1], **Joseph C. Genereux**, and **R. Luke Wiseman**[2]
Department of Molecular & Experimental Medicine, Department of Chemical Physiology, The Scripps Research Institute, La Jolla, CA 92037, USA

SUMMARY

Stress-regulated signaling pathways protect mitochondrial proteostasis, and thus mitochondrial function, from pathologic insults. Despite the importance of stress-regulated signaling pathways in mitochondrial proteome maintenance, the molecular mechanisms by which these pathways maintain mitochondrial proteostasis remain largely unknown. Here, we identify Tim17A as a stress-regulated subunit of the Translocase of the Inner Membrane 23 (TIM23) mitochondrial protein import complex. We show that Tim17A protein levels are decreased downstream of stress-regulated translational attenuation induced by eIF2α phosphorylation through a mechanism dependent on the mitochondrial protease YME1L. Furthermore, we demonstrate that decreasing Tim17A protein levels attenuates TIM23-dependent protein import, promotes the induction of mitochondrial Unfolded Protein Response-associated proteostasis genes, and confers stress-resistance in *C. elegans* and mammalian cells. Thus, our results indicate that Tim17A degradation is a stress-responsive mechanism by which cells adapt mitochondrial protein import efficiency and promote mitochondrial proteostasis in response to the numerous pathologic insults that induce stress-regulated translation attenuation.

Keywords

Tim17A; TIM23; mitochondrial protein import; eIF2α phosphorylation; stress-signaling; mitochondrial proteostasis

INTRODUCTION

Maintaining mitochondrial protein homeostasis (or proteostasis) in response to stress is critical to prevent the pathologic mitochondrial dysfunction associated with numerous human diseases (Baker et al., 2011; Nunnari and Suomalainen, 2012; Rugarli and Langer, 2012). A primary mechanism by which cells maintain mitochondrial proteostasis is through the activation of stress-responsive signaling pathways (Haynes and Ron, 2010; Ryan and Hoogenraad, 2007). These pathways function by adapting the composition and activity of mitochondrial protein import, folding, and proteolytic pathways to prevent the accumulation

[2]Corresponding Author: R. Luke Wiseman, The Scripps Research Institute, 10550 N. Torrey Pines Rd., MEM 220, La Jolla, CA 92037, Phone: (858) 784-8820, Fax: (858) 784-8891, wiseman@scripps.edu.
[1]These authors contributed equally to this work.

Additional Materials and Methods are included in the Supplemental Information.

of misfolded proteins within the mitochondrial environment that can lead to pathologic mitochondrial dysfunction.

A prominent mitochondrial stress-responsive signaling pathway is the mitochondrial unfolded protein response (UPR^{mt}) (Haynes and Ron, 2010; Ryan and Hoogenraad, 2007). The UPR^{mt} is activated by the accumulation of misfolded proteins within the mitochondrial matrix and functions through the transcriptional upregulation of nuclear-encoded proteins involved in mitochondrial proteostasis including chaperones, proteases, and components of mitochondrial protein import pathways (Aldridge et al., 2007; Nargund et al., 2012; Zhao et al., 2002). UPR^{mt} activation is critical for maintaining mitochondrial proteostasis during development and is essential for lifespan extension induced by electron transport chain perturbations in *C. elegans* (Baker et al., 2012; Durieux et al., 2011). The mechanism of UPR^{mt} signaling has primarily been elucidated in *C. elegans* and requires both mitochondrial and cytosolic proteins including the mitochondrial protease CLPP-1, the ABC transporter HAF-1 and the bZIP transcription factor ATFS-1 (Haynes et al., 2007; Haynes et al., 2010). While the mechanism of mammalian UPR^{mt} activation remains poorly characterized, mammalian UPR^{mt} target genes have been identified (Aldridge et al., 2007; Zhao et al., 2002).

Mitochondrial proteostasis is also regulated by other stress-responsive signaling mechanisms such as the integrated stress response (ISR). The ISR is a collective term for the network of stress-regulated kinases (PERK, GCN2, PKR, and HRI) that phosphorylate the α subunit of eukaryotic initiation factor 2 (eIF2α) in response to pathologic insults such as endoplasmic reticulum (ER) stress, amino acid starvation, viral infection, oxidative stress and heme deficiencies (Wek and Cavener, 2007; Wek et al., 2006). Phosphorylation of eIF2α induces translational attenuation of new protein synthesis and activates stress-responsive transcription factors such as activating transcription factor 4 (ATF4) (Harding et al., 2000). The ISR has a critical role in regulating mitochondrial function during stress. Deletion of the ISR kinase GCN-2 sensitizes *C. elegans* to mitochondrial stress and impairs lifespan extension mediated by genetic perturbations of mitochondrial function (Baker et al., 2012). Similarly, genetic inhibition of eIF2α phosphorylation in mice results in significant mitochondrial damage in pancreatic β cells (Back et al., 2009). The ISR-activated transcription factor ATF4 also directly regulates mitochondrial proteostasis through the transcriptional upregulation of proteins involved in mitochondrial proteome maintenance (Harding et al., 2003).

Adapting mitochondrial protein import pathways is also an important mechanism for regulating mitochondrial proteostasis and function during stress. Mitochondrial protein import complexes such as the Translocase of the Outer Membrane (TOM) and Translocase of the Inner Membrane 23 (TIM23) are responsible for the posttranslational import of the >99% of mitochondrial proteins encoded by the nuclear genome (Chacinska et al., 2009; Schmidt et al., 2010). Despite the importance of these complexes in establishing the mitochondrial proteome, the mechanisms by which these complexes are regulated remain poorly understood. The yeast TOM complex is regulated by cytosolic kinases, providing a mechanism to adapt TOM assembly and activity in response to metabolic stress (Schmidt et al., 2011). In human cells, posttranslational degradation of the core TIM23 subunit Tim23 contributes to caspase independent cell death following chronic stress (Goemans et al., 2008) and the expression of the mammalian TIM23 subunit Tim17A is induced by the mitochondrial unfolded protein response (UPR^{mt}) (Aldridge et al., 2007). Furthermore, activation of the UPR^{mt}-associated transcription factor ATFS-1 in *C. elegans* requires stress-induced reduction in TIM23-dependent ATFS-1 import (Nargund et al., 2012).

Here, we characterize the impact of stress on the composition of mammalian TIM23 – the translocase responsible for importing two-thirds of the mitochondrial proteome across the inner mitochondrial membrane into the mitochondrial matrix (Chacinska et al., 2009; Schmidt et al., 2010). We show that the core TIM23 subunit Tim17A is selectively decreased in response to cellular insults that induce translational attenuation through ISR-dependent eIF2α phosphorylation. The stress-regulated decrease in Tim17A involves both reduced Tim17A biogenesis and increased targeting of Tim17A to the mitochondrial protease YME1L for degradation. We show that RNAi-depletion of *TIM17A* attenuates TIM23 protein import efficiency, indicating that stress-dependent reduction in Tim17A decreases mitochondrial protein import. Furthermore, we find that RNAi-depletion of *TIM17A* in mammalian cells or the *TIM17A* homolog, *tim-17*, in *C. elegans* induces expression of stress-responsive mitochondrial proteostasis genes and confers stress-resistance against oxidative insult. Collectively, our results indicate that Tim17A is a stress-regulated TIM23 subunit whose proteins levels are decreased by protective ISR activation, revealing a stress-responsive mechanism to adapt mitochondrial protein import and protect mitochondrial function during pathologic insult.

RESULTS

Tim17A is a Stress-Sensitive TIM23 Subunit Whose Protein Levels Decrease Downstream of ISR Activation

The subunit composition of the mammalian TIM23 import complex is nearly identical to that of yeast, although mammals encode two homologs of the yeast Tim17 subunit: Tim17A and Tim17B. *TIM17A* and *TIM17B* are expressed ubiquitously in mammals, however they demonstrate tissue-specific expression profiles with *TIM17A* enriched in the brain and *TIM17B* enriched in skeletal muscle (Bauer et al., 1999). While no functional differences between Tim17A and Tim17B are currently known, *TIM17A* is a transcriptional target of the mammalian UPR[mt], suggesting that these two Tim17 homologs are differentially regulated during stress (Aldridge et al., 2007).

Using quantitative immunoblotting, we found that the environmental toxin arsenite (As(III)) induces a rapid decrease of Tim17A in HEK293T cells, demonstrating a half-time (t_{50}) of ~2 h (Figure 1A,B Neither Tim17B nor Tim23 were affected over the timecourse of this experiment. Tim17A was highly sensitive to As(III) in HEK293T cells, demonstrating reduced protein levels at As(III) concentrations as low as 5 μM (Figure S1A). Similar results were observed in all cell lines tested including SHSY5Y, Hela, and Huh7 (Figure S1B–D). As(III) also decreased Tim17A protein levels in retinoic-acid differentiated SHSY5Y cells (Figure S1E), indicating that the observed effect occurs in post-mitotic cells.

As(III) is a potent activator of the ISR (McEwen et al., 2005). This is shown by the transient increase in eIF2α phosphorylation in As(III)-treated HEK293T cells (Figure 1A). This transient increase in phosphorylated eIF2α results from the ISR-dependent induction of the eIF2α phosphatase regulatory subunit GADD34 in a negative feedback loop of ISR signaling (Novoa et al., 2001). We evaluated whether As(III)-dependent reductions in Tim17A could be attributed to ISR activation using wild-type mouse embryonic fibroblasts (MEF[WT]) and knockin MEFs expressing the S51A eIF2α mutant (MEF[A/A]) (Scheuner et al., 2001). The S51A eIF2α mutant is refractory to stress-induced eIF2α phosphorylation, preventing ISR activation (Scheuner et al., 2001). MEF[WT] demonstrate a 60% decrease in Tim17A in response to As(III) (Figure 1C,D). Tim23 protein levels were also decreased in As(III)-treated MEF[WT], albeit to a lower extent. Alternatively, we observed a significant *increase* in Tim17A and Tim23 protein levels in As(III)-treated MEF[A/A], indicating that As(III)-dependent reductions in Tim17A require eIF2α phosphorylation. The similar levels of phosphorylated eIF2α in control and As(III)-treated MEF[WT] (Figure 1C) reflects the

transient increase in eIF2α phosphorylation mediated by the ISR-dependent increase in GADD34 (Novoa et al., 2001). A timecourse of As(III)-treatment in MEF[WT] shows this As(III)-dependent, transient increase in eIF2α phosphorylation (Figure S1F).

We used a HEK293 cell line stably expressing the ligand-activated eIF2α kinase Fv2e-PERK (Lin et al., 2009; Lu et al., 2004) to evaluate whether stress-independent ISR activation decreases Tim17A. Fv2e-PERK kinase activity is activated by the addition of the ligand AP20187, increasing eIF2α phosphorylation. The addition of AP20187 significantly reduced Tim17A in Fv2e-PERK expressing cells (Figure 1E). Neither Tim17B nor Tim23 were affected by Fv2e-PERK activation. AP20187 did not influence Tim17A in control cells that do not express Fv2e-PERK. AP20187-dependent Fv2e-PERK activation rapidly decreases Tim17A protein levels at a rate similar to that observed for As(III) (Figure S1G).

The ISR is activated by a variety of pathologic insults including ER stress (Wek and Cavener, 2007; Wek et al., 2006), which should similarly decrease Tim17A. Tim17A protein levels are reduced in MEF[WT] treated with the ER stress-inducer thapsigargin (Tg) (Figure 1F,G) – a small molecule SERCA inhibitor that increases eIF2α phosphorylation through activation of the endogenous eIF2α kinase PERK as part of the ER unfolded protein response (Harding et al., 2002; Schroder and Kaufman, 2005). Tim17A was not affected in Tg-treated MEF[A/A]. Tg did not influence Tim23 levels in either MEF[A/A] or MEF[WT]. The transient Tg-dependent increase in eIF2α phosphorylation observed in MEF[WT] reflects the GADD34 negative feedback loop of ISR signaling (Figure 1F) (Novoa et al., 2001). Tg also reduced Tim17A in HEK293T cells (Figure S1H). These results further confirm the sensitivity of Tim17A to ISR activation.

ISR-dependent reductions in Tim17A could be afforded by ISR-mediated translational attenuation or the increased expression of stress-responsive genes such as a protease induced by stress-regulated transcription factors activated by the ISR (e.g. ATF4)(Harding et al., 2000; Harding et al., 2003; Vattem and Wek, 2004). We explored the contributions of these two potential mechanisms by monitoring the stress-induced decrease of Tim17A in cells treated with the ribosomal translation inhibitor cycloheximide (CHX). CHX decreases Tim17A independent of stress in HEK293T cells (Figure S1I). Neither Tim17B nor Tim23 were significantly affected by CHX. CHX reduces Tim17A in both MEF[WT] and MEF[A/A] (Figure 1H), demonstrating that CHX decreases Tim17A independent of eIF2α phosphorylation. CHX is known to increase eIF2α phosphorylation (Jiang et al., 2003) (shown in the CHX-treated MEF[WT] cell; Figure 1H), but CHX prevents translation of ISR induced stress-responsive genes. The sensitivity of Tim17A to CHX indicates that the ISR-dependent decrease in Tim17A is most likely attributed to reductions in cytosolic protein synthesis and not the ISR-dependent increase in a stress-responsive protein(s).

Stress-Dependent Reductions in Tim17A are Mediated by Decreased Tim17A Biogenesis and Increased Targeting of Tim17A to Proteolytic Degradation

To explore the mechanism of stress-dependent reductions in Tim17A, we initially measured *TIM17A* mRNA in As(III)-treated HEK293T cells using qPCR (Figure 2A). As(III) increased *TIM17A* mRNA levels in these cells following a 6 h treatment, consistent with *TIM17A* being a stress-responsive gene (Aldridge et al., 2007). The mRNA of the stress-responsive *HSP60* was similarly induced by As(III), while *TIM23* was not. *TIM17A* mRNA decreased to basal levels following 12 h As(III)-treatment. Other ISR activators including Tg also induced *TIM17A* in MEF[WT] cells (Figure S2A). These results show that the As(III)- or Tg-dependent reduction in Tim17A cannot be attributed to decreased *TIM17A* mRNA.

We used [^{35}S] metabolic labeling to measure the impact of As(III) on Tim17A biogenesis, a process including protein translation, mitochondrial import, and incorporation into the

mitochondrial inner membrane (Kaldi et al., 1998). We pre-treated HEK293T with As(III) prior to labeling with [^{35}S]-Met/Cys (Figure 2B). Tim17A was immunopurified from these samples and the amount of newly-synthesized [^{35}S]-labeled Tim17A was measured by autoradiography. Tim17A biogenesis was reduced to 25% of control levels following a 2 h As(III) pre-treatment (Figure 2B,C), consistent with the reduced translation afforded by As(III)-dependent ISR activation (Wek and Cavener, 2007; Wek et al., 2006). Following 4 or 6 h As(III) pretreatment, Tim17A levels were restored to 60% or 40% of control levels, respectively, reflecting, at least in part, the restoration of ribosomal translation afforded by ISR-dependent increases in GADD34 (Novoa et al., 2001).

We also measured the rate of Tim17A degradation in As(III)-treated cells using [^{35}S] metabolic labeling. HEK293T labeled with [^{35}S]-Met/Cys were chased with nonradioactive media in the presence or absence of As(III) (Figure 2D). Tim17A was immunopurified from these cells at varying times, allowing direct measurement of Tim17A degradation. In the absence of As(III), [^{35}S]-labeled Tim17A has an intracellular half-life ($t_{1/2}$) of ~6 h (Figure 2D,E). The addition of As(III) to the chase media reduced the $t_{1/2}$ for [^{35}S]-labeled Tim17A to 2 h, a $t_{1/2}$ nearly identical to the t_{50} for As(III)-dependent reductions in Tim17A observed by quantitative immunoblotting (**c.f.** Figure 1B and 2E). This shows that As(III) decreases Tim17A intracellular stability and increases Tim17A degradation. The addition of CHX to the chase media similarly reduced Tim17A intracellular stability and increased Tim17A degradation (Figure 2F,G). As a control, we show that the stability of the global [^{35}S]-labeled proteome was not affected by CHX (Figure S2B,C).

Collectively, the above results are consistent with a mechanism where translational attenuation reduces Tim17A protein levels through both reductions in Tim17A biogenesis and increased targeting of Tim17A to proteolytic degradation (Figure 2H).

Stress-Regulated Tim17A Degradation Requires the i-AAA Protease YME1L

We sought to identify the protease responsible for Tim17A degradation. We monitored Tim17A stability in isolated mitochondria purified from HEK293T cells. Tim17A is stable in isolated mitochondria incubated in the absence of ATP (Figure 3A). The addition of ATP significantly reduced Tim17A protein levels (Figure 3A). The ATP-dependent decrease in Tim17A could be inhibited by the membrane permeable zinc chelator *o*-phenanthroline (o-phe), suggesting that Tim17A degradation requires the activity of a mitochondrial-localized ATP-dependent zinc metalloprotease.

Mitochondrial inner membrane proteins are primarily degraded by three constitutively active, ATP-dependent AAA+ zinc metalloproteases localized to the inner mitochondrial membrane: YME1L, AFG3L2, and paraplegin (Koppen and Langer, 2007; Tatsuta, 2009). The primary difference between these three ATP-dependent metalloproteases is the localization of their proteolytic activity. The active site for the *i*-AAA protease YME1L is oriented to the IMS, while the active sites for the *m*-AAA proteases AFG3L2 and paraplegin are oriented towards the mitochondrial matrix.

We evaluated the dependence of Tim17A degradation on the *i*-AAA protease YME1L using shRNA. The knockdown of *YME1L* significantly impaired As(III)- and CHX-dependent Tim17A degradation (Figure 3B,C). Genetic depletion of *AFG3L2* did not impair CHX-dependent Tim17A degradation (Figure S3). The ATP-dependent degradation of Tim17A was also attenuated in mitochondria isolated from cells depleted of *YME1L* (Figure 3D), further demonstrating that Tim17A degradation requires YME1L.

YME1L-dependent Tim17A degradation could occur while Tim17A remains in complex with TIM23 or following stress-induced dissociation from TIM23. We differentiated these

two potential mechanisms by measuring the impact of As(III) on the interaction between the core TIM23 subunits Tim23 and Tim17A or Tim17B. We immunopurified Tim23 from digitonin-permeabilized mitochondria isolated from SHSY5Y cells treated with or without As(III) and measured the co-immunopurification of Tim17A and Tim17B by immunoblotting (Geissler et al., 2002). Both Tim17A and Tim17B co-immunopurify with Tim23 in mitochondria isolated from untreated cells (Figure 4A)(Bauer et al., 1999). Alternatively, only Tim17B co-immunopurifies with Tim23 in mitochondria isolated from As(III)-treated cells, indicating that the rapid decrease in Tim17A protein levels reduces the population of TIM23 with a core Tim23-Tim17A interaction, but does not significantly influence TIM23 with a Tim23-Tim17B core. Similar results were observed by Blue-Native (BN)-PAGE where the size of the TIM23 core complex (containing Tim23-Tim17A/B) is not significantly affected by As(III), although we do observe a 35% decrease in TIM23 (Figure 4B). This decease in TIM23 complexes is consistent with the selective loss of TIM23 complexes containing a core Tim23-Tim17A interaction.

We next evaluated whether As(III) affected the Tim23-Tim17A interaction by immunopurifying Tim23 from As(III)-treated HEK293T cells RNAi-depleted of *YME1L* (cells deficient in stress-induced Tim17A degradation). Tim17A efficiently co-immunopurifies with Tim23 in control and As(III)-treated HEK239T cells RNAi-depleted of *YME1L* (Figure 4C), indicating that As(III) does not induce Tim17A dissociation from Tim23. This result strongly suggests that YME1L-dependent Tim17A degradation is initiated while Tim17A remains in complex with TIM23.

Stress-dependent increases in YME1L-dependent Tim17A degradation could result from stress-dependent alterations in YME1L proteolytic activity. While yeast Yme1 is known to be in close proximity with TIM23 (Rainey et al., 2006), we did not recover YME1L in our Tim23 immunopurifications in the presence or absence of As(III), indicating that As(III) does not induce a stable interaction between mammalian YME1L and TIM23 (Figure 4C). We also did not observe significant alterations in YME1L oligomeric size induced by As(III), as measured by BN-PAGE (Figure 4D), suggesting that As(III) does not increase or decrease YME1L interactions with regulatory adaptor proteins, such as those identified for yeast Yme1 (Dunn et al., 2006; Dunn et al., 2008). Since no adaptors for mammalian YME1L have been identified to date and YME1L is not known to be posttranslationally regulated (Koppen and Langer, 2007; Tatsuta, 2009), our results suggest that As(III) does not alter YME1L proteolytic activity towards Tim17A, although we cannot explicitly exclude the possibility that As(III) induces conformational changes within YME1L through other mechanisms such as posttranslational modification (e.g. phosphorylation) or transient interaction with unidentified adaptor proteins.

Reduced Tim17A Attenuates TIM23-Dependent Mitochondrial Protein Import

The As(III)-dependent decrease in TIM23 complexes containing Tim17A (Figure 4A,B) will decrease cellular mitochondrial protein import efficiency by reducing the population of functional complexes containing the essential 1:1 interaction between Tim23 and either Tim17A or Tim17B (Bauer et al., 1999; Chacinska et al., 2009; Schmidt et al., 2010). We measured the impact of As(III) on the mitochondrial import of a C-terminally HA tagged ornithine transcarbamylase (OTC[HA]) and a monomeric transthyretin variant (M-TTR; (Jiang et al., 2001)) targeted to the mitochondrial matrix by an N-terminal CoxVIII mitochondrial targeting sequence ([mt]M-TTR). We employed M-TTR as a model TIM23 substrate as M-TTR is a well-established soluble protein that has no biochemical activity that can disrupt mitochondrial function. Mitochondrial matrix populations of OTC[HA] and [mt]M-TTR can be identified by their increased mobility on SDS-PAGE afforded by the cleavage of their

mitochondrial targeting sequences by mitochondrial-localized processing peptidase (Gakh et al., 2002) (Figure S4A,B).

Using the differential mobility of mitochondrial-localized OTC[HA] and [mt]M-TTR observed by SDS-PAGE, we monitored the impact of As(III) on mitochondrial protein import efficiency using [^{35}S] metabolic labeling (Figure 5A,B). Cells pretreated with or without As(III) were labeled with [^{35}S] prior to immunopurification of OTC[HA] or [mt]M-TTR. Import efficiency was then quantified by measuring the mitochondrial fraction of [^{35}S]-labeled OTC[HA] and [mt]M-TTR. Pretreatment with As(III) decreased the mitochondrial import of OTC[HA] (Figure 5A) and [mt]M-TTR (Figure 5B). Mitochondrial import of these proteins was also reduced when the uncoupling agent CCCP (an efficient inhibitor of mitochondrial protein import) was co-administered during the pulse. The As(III)-dependent reduction in mitochondrial protein import cannot be attributed to depolarization of the mitochondrial membrane, as we did not observe significant alterations in mitochondrial membrane potential in As(III)-treated cells measured by TMRE fluorescence (Figure S4C).

We next evaluated the impact of genetic depletion of *TIM17A* on the import of [mt]M-TTR in HEK293TRex cells. We confirmed >90% knockdown of Tim17A in these cells by immunoblotting (Figure 5C). *TIM17A* depletion did not significantly influence Tim17B or Tim23 protein levels. Genetic depletion of *TIM17A* reduced the import efficiency of [mt]M-TTR by ~25% (Figure 5D). This effect could not be attributed to alterations in total protein production as the total amount of [^{35}S]-labeled [mt]M-TTR was nearly identical in HEK293T-REX cells expressing control or *TIM17A* shRNA (Figure S4D). Furthermore, the reduction in [mt]M-TTR import cannot be attributed to a reduction in mitochondrial membrane potential afforded by *TIM17A*-depletion, as reduced Tim17A does not influence the mitochondrial membrane potential measured by TMRE fluorescence (Figure S4E).

Alterations in mitochondrial protein import afforded by *TIM17A* depletion could directly impact mitochondrial proteome composition. We measured the impact of *TIM17A* depletion on the mitochondria proteome using quantitative Multi-Dimensional Protein Identification Technology (MuDPIT) proteomics (Yates et al., 2009). Enriched mitochondria isolates from cells expressing control or *TIM17A* shRNA were trypsinized, labeled with distinct Tandem Mass Tags (TMTs), and analyzed by the LC/LC-MS/MS MuDPIT protocol (Washburn et al., 2001). The composition of mitochondrial proteomes from these two preparations were directly compared by measuring the recovery of differentially TMT-labeled peptides. We identified 317 GO-annotated mitochondrial proteins (Figure 5E, Table S1). *TIM17A* depletion did not significantly influence the global composition of the mitochondrial proteome, although we cannot explicitly rule out alterations in protein levels for mitochondrial proteins not detected in the MuDPIT analysis.

Reduced TIM17A/tim-17 Increases Expression of Stress-Responsive Mitochondrial Proteostasis Genes and Confers Stress-Resistance in Mammalian Cells and C. elegans

Reducing TIM23 import efficiency leads to the activation of the UPR[mt] in *C. elegans* (Nargund et al., 2012). This suggests that reducing TIM23 import efficiency by depleting the worm *TIM17A* homolog, *tim-17* (E04A4.5), should induce the UPR[mt]. Consistent with this prediction, N2 wild-type worms expressing the UPR[mt] reporter *hsp-60$_{pr}$::gfp* fed bacteria expressing *tim-17(RNAi)* demonstrated a robust increase in GFP fluorescence, reflecting UPR[mt] activation. The activation of the UPR[mt] by *tim-17(RNAi)* was independent of mitochondrial matrix stress, as *tim-17(RNAi)* significantly activated *hsp-60::gfp* in a HAF-1 mutant worm (*haf-1(ok705)*) (Figure 6A) – HAF-1 is an ABC peptide transporter required for UPR[mt] activation in response to mitochondrial matrix stress (Haynes et al., 2010). Alternatively, *tim-17(RNAi)* did not increase *hsp-60$_{pr}$::gfp* expression in worms expressing a mutant of the UPR[mt] transcription factor ATFS-1 (*atfs-1(tm4525)*), indicating

that *tim-17(RNAi)*-dependent UPR^{mt} activation requires ATFS-1 (Figure 6A). The UPR^{mt} activation induced by *tim-17(RNAi)* is identical to that previously observed with *tim-23(RNAi)* (Nargund et al., 2012)(Figure 6A).

Although the mammalian UPR^{mt} remains poorly characterized, we anticipated that depletion of *TIM17A* would increase expression of mammalian mitochondrial stress-responsive genes such as the chaperonin *HSP60* and the protease *YME1L* (Aldridge et al., 2007). We observed a modest increase in *HSP60* and *YME1L* mRNA in HEK293T cells RNAi-depleted of *TIM17A* (Figure 6B). Similar results were observed in *TIM17A*-depleted SHSY5Y cells (Figure S5). While the modest increase in expression of these genes is consistent with previous reports measuring mammalian UPR^{mt} activation (Aldridge et al., 2007; Zhao et al., 2002), other stress-responsive inputs (e.g. activation of a stress-responsive transcription factor) may also be required for a robust UPR^{mt} activation in mammalian cells.

The induction of mitochondrial stress-responsive genes afforded by reduced TIM23 import efficiency should increase organismal stress-resistance against pathologic insults that challenge mitochondrial proteostasis. We explore this prediction in *C. elegans* treated with the superoxide generator paraquat – a stress that disrupts *C. elegans* mitochondrial proteostasis (Nargund et al., 2012; Runkel et al., 2013). Wild-type N2 worms fed *tim-17(RNAi)* demonstrated a significant increase in stress-resistance against the toxin paraquat (Figure 6C). Similar stress-resistance was observed in worms fed *tim-23(RNAi)*. Surprisingly, *tim-17(RNAi)* and *tim-23(RNAi)* increased paraquat stress-resistance in *atfs-1(tm4525)* mutant worms, indicating that the increased paraquat stress-resistance afforded by reduced TIM23 import activity is not solely dependent on activation of the UPR^{mt}-associated transcription factor ATFS-1 (Figure 6D). *TIM17A* depletion in HEK293T also results in a modest, but statistically significant, increase in paraquat stress resistance (Figure 6E). These results indicate that reducing Tim17A protein levels increases cellular and organismal resistance to oxidative insult.

DISCUSSION

Here, we identify Tim17A as a stress-regulated subunit of the TIM23 import complex (Figure 7). We show that Tim17A protein levels are significantly decreased downstream of protective, ISR-mediated translational attenuation. Furthermore, we show that reduction in Tim17A attenuates mitochondrial protein import, increases transcription of mitochondrial proteostasis genes, and confers stress-resistance against oxidative insult. Thus, our results indicate that reductions in Tim17A afforded by stress-regulated translational attenuation provides a mechanism to adapt mitochondrial protein import and increase cellular stress resistance during pathologic insults.

Stress-dependent reductions in Tim17A result from a decrease in Tim17A biogenesis and an increase in Tim17A degradation. While the decrease in Tim17A biogenesis can be largely explained by reductions in Tim17A synthesis during ISR-dependent translational attenuation (Wek and Cavener, 2007; Wek et al., 2006), the increased degradation of Tim17A observed following CHX treatment suggests that Tim17A stability is sensitive to alterations in new protein synthesis. One potential mechanism to explain this decreased Tim17A stability is that reductions in new protein synthesis directly influence the conformation of Tim17A within the TIM23 complex. The 'opening' of the TIM23 channel requires the presence of newly-synthesized proteins containing an N-terminal mitochondrial targeting sequence (Chacinska et al., 2009; Schmidt et al., 2010). Therefore, reductions in new protein synthesis will result in less TIM23 'opening'. Since Tim17A directly associates with the channel forming subunit Tim23, the decreased capacity for TIM23 to open during translation attenuation could induce conformational conversions within Tim17A that lead to increased

degradation. This mechanism is consistent with our results demonstrating that Tim17A does not dissociate from Tim23 during stress, indicating that Tim17A degradation is initiated while it remains in complex with TIM23. While the relationship between Tim17A stability and reduced translation remains to be further elucidated, our results clearly show that the sensitivity of Tim17A to stress-regulated translational attenuation reveals a cellular mechanism to adapt TIM23 import efficiency and promote mitochondrial proteostasis during stress.

The capacity to regulate mitochondrial protein import through stress-regulated decreases in Tim17A provides a mechanism to promote proteostasis remodeling in mammalian cells through the UPR[mt]. In *C. elegans*, reductions in TIM23 import are required for UPR[mt] activation (Nargund et al., 2012), although the biologic mechanisms that reduce import during stress are currently unknown. We show that reductions in Tim17A decrease mitochondrial protein import efficiency and increase expression of known mammalian UPR[mt] target genes, suggesting that stress-regulated Tim17A degradation is a biologic mechanism that can regulate mitochondrial import and promote UPR[mt] activation in mammalian cells. Consistent with this prediction, the UPR[mt]-dependent upregulation of *TIM17A* allows restoration of Tim17A following stress through a negative feedback loop (a common feature of stress-regulated signaling pathways).

Our results also suggest a cooperative interaction between ISR-dependent reductions in Tim17A and UPR[mt] activation (Figure 7). This potential role for the ISR in UPR[mt] activation is conceptually similar to that employed to activate NF-κB in response to UV irradiation, where the ISR-dependent reduction in IκB synthesis contributes to the decreased intracellular levels of this inhibitory protein and facilitates NF-κB activation (Jiang and Wek, 2005; Wu et al., 2004). While ISR-dependent Tim17A degradation represents one potential mechanism to attenuate mitochondrial protein import and activate the UPR[mt], other mechanisms are likely employed for UPR[mt] activation in response to proteotoxic imbalances in the mitochondrial matrix, explaining the involvement of the mitochondrial matrix protease CLPP-1 and the peptide transporter HAF-1 in UPR[mt] activation in response to these types of stresses (Haynes et al., 2007; Haynes et al., 2010).

Interestingly, we also show that reduced TIM23 import efficiency increases organismal stress-resistance through mechanisms independent of the UPR[mt]-associated transcription factor ATFS-1(Figure 7). Altering mitochondrial protein import has previously been shown to be beneficial for promoting mitochondrial function in response to stress. PKA-dependent phosphorylation of the TOM subunit Tom70 decreases the import of mitochondrial metabolite carriers in non-respiring conditions, adapting mitochondrial protein import (and thus function) to the metabolic state of the cell (Schmidt et al., 2011). Although we did not identify significant alterations in the composition of mitochondrial proteomes in *TIM17A*-depleted cells, reductions in Tim17A may alter the import of specific mitochondrial proteins not identified in our proteomic analysis, providing a mechanism to adapt mitochondrial function in response to pathologic insults that induce ISR activation. Alternatively, reductions in TIM23 import efficiency afforded by reduced Tim17A could function to reduce the burden of newly-synthesized proteins entering the mitochondrial matrix during conditions of stress. Newly-synthesized, unfolded polypeptides are the predominant substrates for mitochondrial folding and proteolytic pathways. Therefore, reducing the population of these proteins entering the mitochondrial matrix during stress would increase the available capacity for mitochondrial proteostasis pathways to maintain mitochondrial proteome integrity and prevent the pathologic accumulation of misfolded proteins within the mitochondrial matrix. This mechanism is analogous to the reduced burden on cellular proteostasis pathways afforded by ISR-dependent translational attenuation (Wek and Cavener, 2007; Wek et al., 2006) and suggests that altering the import rate of newly-

synthesized mitochondrial proteins entering the matrix is a mechanism to selectively promote mitochondrial proteostasis during stress.

While *TIM17A* and *TIM17B* are ubiquitously expressed (Bauer et al., 1999), the tissue-selective expression of these proteins and their differential sensitivities to stress-regulated translational attenuation suggests unique requirements for TIM23 import regulation in different tissues. Tim17B is stable during stress, suggesting a more housekeeping role for this Tim17 homolog. The stability of Tim17B, and thus mitochondrial import activity, could be important for tissues such as skeletal muscle that express high levels of *TIM17B*, providing a mechanism to ensure efficient mitochondrial protein import to maintain the high metabolic activities required of these tissues during stress. Alternatively, the stress-sensitivity of Tim17A suggests that tissues that selectively express *TIM17A* such as the brain are highly dependent on TIM23 import regulation to promote mitochondrial proteostasis during pathologic insults. Thus, the tissue-specific requirements for TIM23 import activity could reflect the evolutionary advantage for metazoans having two Tim17 homologs, while yeast only require one Tim17 (Chacinska et al., 2009).

Mitochondrial proteome maintenance is critical to ensure organismal viability in response to environmental, genetic or aging-related stress. Thus, determining cellular stress-resistance pathways involved in adapting mitochondrial proteostasis in response to pathologic insults is critical. Here, we identify Tim17A as a stress-regulated subunit of the TIM23 mitochondrial protein import complex whose protein levels decrease downstream of ISR-mediated translation attenuation. Identifying Tim17A as a stress-regulated mitochondrial import component provides insight into the coordination of stress-responsive signaling cascades in defining mitochondrial function during stress and reveals previously unanticipated therapeutic targets (e.g. ISR signaling) to adapt mitochondrial protein import and potentially attenuate mitochondrial dysfunction in human disease pathology.

EXPERIMENTAL PROCEDURES

Cell Culture

HEK293T, HeLa, and Huh7 cells were cultured in DMEM (Cellgro) supplemented with 10% fetal bovine serum (Cellgro), 1% penicillin/streptomycin (Gibco) and 1% L-glutamine (Cellgro) at 37°C (5% CO_2). MEF^{WT} and MEF$^{A/A}$ cells were cultured as above and supplemented with β-mercaptoethanol. SHSY5Y cells were cultured in DMEM/F12 (Cellgro) supplemented with 10% fetal bovine serum (Cellgro), 1% penicillin/streptomycin (Gibco) and 1% L-glutamine (Gibco).

Cell Lysis and Immunoblotting

Cellular lysates were prepared using a standard Lysis Buffer (20 mM Hepes pH 7.5 100 mM NaCl 1 mM EDTA 1% Triton supplemented with EDTA-free protease inhibitors (Roche)). Cellular lysates were normalized by total protein concentration using Bio-Rad protein quantification. Lysates were separated on Tris-glycine gels and transferred onto nitrocellulose membranes (Bio-Rad) for immunoblotting. Following incubation with primary antibodies, membranes were incubated with IR-labeled secondary antibodies (Li-COR Biosciences) and analyzed using the Odyssey Infrared Imaging System (Li-COR Biosciences).

[^{35}S] Metabolic Labeling

Metabolic labeling was achieved using 20 μCi/mL [^{35}S]-TRANSlabel (ICN) in DMEM lacking methionine and cysteine (Cellgro) supplemented with 10% dialyzed serum. Following labeling, cells were incubated in complete media, as indicated. At the indicated

time, cellular lysates were prepared in Lysis Buffer and denatured using 1% SDS and boiling for 5 min at 100 °C. The denatured lysates were diluted 1:10 into RIPA buffer lacking SDS (50 mM Tris pH 7.5 150 mM NaCl, 0.5% sodium deoxycholate, 1% NP-40) and cleared using quenched sepharose. Tim17A was immunoprecipitated using α-Tim17(H-1) antibody (Santa Cruz) conjugated to Protein G sepharose (Invitrogen). Following stringent washing in RIPA buffer, Tim17A was eluted by boiling in Laemmli buffer, separated on SDS-PAGE and analyzed by autoradiography using a Typhoon Trio Imager (GE Healthcare).

Mitochondrial Isolation and Immunopurification of the TIM23 complex

Mitochondria were isolated from cells using a previously reported mitochondrial isolation protocol (Haynes et al., 2010). Freshly isolated mitochondria were resuspended in Mitochondrial Import Buffer (25 mM HEPES●KOH pH 7.4, 250 mM sorbitol, 150 mM KCl, 10 mM $MgCl_2$, 2 mM K_2PO_4) supplemented with 5 mM malate, 10 mM pyruvate, 20 mM succinate and incubated at 37 °C in the presence or absence of 5 mM ATP and 1 mM *o*-phenanthroline, as indicated. Mitochondria were then collected by centrifugation, lysed in Lysis Buffer and analyzed by immunoblotting.

Immunoprecipitation of the TIM23 complex was carried out as described in (Geissler et al., 2002) using Tim23 antibody (BD Transduction Laboratories) pre-coupled to Protein G Sepharose beads (GE Healthcare) and incubating for 3 hours at room temperature. After washing, samples were eluted with Laemmili buffer.

BN-PAGE Analysis

Isolated mitochondrial were resuspended in BN-Lysis buffer (20 mM Tris pH 7.5, 10% (w/v) glycerol, 50 mM NaCl, 0.1 mM EDTA, and 1 mM PMSF), lysed by the addition of digitonin, separated on 4–16% polyacrylamide gels, and western blotted as described (Geissler et al., 2002).

Mitochondrial Protein Import Assay

HEK293T or HEK293T-Rex cells expressing OTC^{HA} or ^{mt}M-TTR were labeled for 30 min using 20 μCi/mL [^{35}S]-TRANSlabel (ICN) in DMEM lacking methionine and cysteine (Cellgro) supplemented with 10% dialyzed serum in the absence or presence of CCCP (50 μM). Cells were then lysed with RIPA buffer and OTC^{HA} or ^{mt}M-TTR was immunopurified using Protein G Sepharose preconjugated to anti-HA (Covance) or Protein A Sepharose preconjugated to a rabbit polyclonal anti-TTR antibody, respectively. Immunopurified proteins were separated by SDS-PAGE and analyzed by autoradiography using a Typhoon Trio Imager (GE Healthcare). Fraction import was calculated using the following equation: mitochondrial [^{35}S]-labeled protein/(cytosolic [^{35}S]-labeled protein + mitochondrial [^{35}S]-labeled protein).

Resazurin Cell Viability Assay

Cells were plated at a density of 10,000 cells per well into black 96-well plates and cultured overnight in cell media. Indicated stressors were introduced to each well in equal volume and incubated for the indicated time. Resazurin was diluted 1:10 into each well (final concentration 50 μM) and incubated for 1 h. Resazurin fluorescence was measured using a SAFIRE 2 fluorescent plate reader (TECAN) with an emission wavelength of 590nm and an excitation wavelength of 560nm. All resazurin assays were performed in triplicate.

Quantitative RT-PCR

The relative mRNA expression levels of *TIM17A*, *TIM23*, and *HSP60* were analyzed by quantitative RT-PCR as described(Shoulders et al., 2013).

Statistical Analyses

Data were analyzed using Students t-test to determine significance. Error bars depict SEM.

Supplementary Material

Refer to Web version on PubMed Central for supplementary material.

Acknowledgments

REFERENCES

Aldridge JE, Horibe T, Hoogenraad NJ. Discovery of genes activated by the mitochondrial unfolded protein response (mtUPR) and cognate promoter elements. PLoS One. 2007; 2:e874. [PubMed: 17849004]

Back SH, Scheuner D, Han J, Song B, Ribick M, Wang J, Gildersleeve RD, Pennathur S, Kaufman RJ. Translation attenuation through eIF2alpha phosphorylation prevents oxidative stress and maintains the differentiated state in beta cells. Cell Metab. 2009; 10:13–26. [PubMed: 19583950]

Baker BM, Nargund AM, Sun T, Haynes CM. Protective coupling of mitochondrial function and protein synthesis via the eIF2alpha kinase GCN-2. PLoS Genet. 2012; 8:e1002760. [PubMed: 22719267]

Baker MJ, Tatsuta T, Langer T. Quality control of mitochondrial proteostasis. Cold Spring Harb Perspect Biol. 2011; 3

Bauer MF, Gempel K, Reichert AS, Rappold GA, Lichtner P, Gerbitz KD, Neupert W, Brunner M, Hofmann S. Genetic and structural characterization of the human mitochondrial inner membrane translocase. J Mol Biol. 1999; 289:69–82. [PubMed: 10339406]

Chacinska A, Koehler CM, Milenkovic D, Lithgow T, Pfanner N. Importing mitochondrial proteins: machineries and mechanisms. Cell. 2009; 138:628–644. [PubMed: 19703392]

Dunn CD, Lee MS, Spencer FA, Jensen RE. A genomewide screen for petite-negative yeast strains yields a new subunit of the i-AAA protease complex. Mol Biol Cell. 2006; 17:213–226. [PubMed: 16267274]

Dunn CD, Tamura Y, Sesaki H, Jensen RE. Mgr3p and Mgr1p are adaptors for the mitochondrial i-AAA protease complex. Mol Biol Cell. 2008; 19:5387–5397. [PubMed: 18843051]

Durieux J, Wolff S, Dillin A. The cell-non-autonomous nature of electron transport chain-mediated longevity. Cell. 2011; 144:79–91. [PubMed: 21215371]

Gakh O, Cavadini P, Isaya G. Mitochondrial processing peptidases. Biochim Biophys Acta. 2002; 1592:63–77. [PubMed: 12191769]

Geissler A, Chacinska A, Truscott KN, Wiedemann N, Brandner K, Sickmann A, Meyer HE, Meisinger C, Pfanner N, Rehling P. The mitochondrial presequence translocase: an essential role of Tim50 in directing preproteins to the import channel. Cell. 2002; 111:507–518. [PubMed: 12437924]

Goemans CG, Boya P, Skirrow CJ, Tolkovsky AM. Intra-mitochondrial degradation of Tim23 curtails the survival of cells rescued from apoptosis by caspase inhibitors. Cell Death Differ. 2008; 15:545–554. [PubMed: 18174902]

Harding HP, Calfon M, Urano F, Novoa I, Ron D. Transcriptional and translational control in the Mammalian unfolded protein response. Annu Rev Cell Dev Biol. 2002; 18:575–599. [PubMed: 12142265]

Harding HP, Novoa I, Zhang Y, Zeng H, Wek R, Schapira M, Ron D. Regulated translation initiation controls stress-induced gene expression in mammalian cells. Mol Cell. 2000; 6:1099–1108. [PubMed: 11106749]

Harding HP, Zhang Y, Zeng H, Novoa I, Lu PD, Calfon M, Sadri N, Yun C, Popko B, Paules R, et al. An integrated stress response regulates amino acid metabolism and resistance to oxidative stress. Mol Cell. 2003; 11:619–633. [PubMed: 12667446]

Haynes CM, Petrova K, Benedetti C, Yang Y, Ron D. ClpP mediates activation of a mitochondrial unfolded protein response in C. elegans. Dev Cell. 2007; 13:467–480. [PubMed: 17925224]

Haynes CM, Ron D. The mitochondrial UPR - protecting organelle protein homeostasis. J Cell Sci. 2010; 123:3849–3855. [PubMed: 21048161]

Haynes CM, Yang Y, Blais SP, Neubert TA, Ron D. The matrix peptide exporter HAF-1 signals a mitochondrial UPR by activating the transcription factor ZC376.7 in C. elegans. Mol Cell. 2010; 37:529–540. [PubMed: 20188671]

Jiang HY, Wek RC. GCN2 phosphorylation of eIF2alpha activates NF-kappaB in response to UV irradiation. Biochem J. 2005; 385:371–380. [PubMed: 15355306]

Jiang HY, Wek SA, McGrath BC, Scheuner D, Kaufman RJ, Cavener DR, Wek RC. Phosphorylation of the alpha subunit of eukaryotic initiation factor 2 is required for activation of NF-kappaB in response to diverse cellular stresses. Mol Cell Biol. 2003; 23:5651–5663. [PubMed: 12897138]

Jiang X, Smith CS, Petrassi HM, Hammarstrom P, White JT, Sacchettini JC, Kelly JW. An engineered transthyretin monomer that is nonamyloidogenic, unless it is partially denatured. Biochemistry. 2001; 40:11442–11452. [PubMed: 11560492]

Kaldi K, Bauer MF, Sirrenberg C, Neupert W, Brunner M. Biogenesis of Tim23 and Tim17, integral components of the TIM machinery for matrix-targeted preproteins. EMBO J. 1998; 17:1569–1576. [PubMed: 9501078]

Koppen M, Langer T. Protein degradation within mitochondria: versatile activities of AAA proteases and other peptidases. Crit Rev Biochem Mol Biol. 2007; 42:221–242. [PubMed: 17562452]

Lin JH, Li H, Zhang Y, Ron D, Walter P. Divergent effects of PERK and IRE1 signaling on cell viability. PLoS One. 2009; 4:e4170. [PubMed: 19137072]

Lu PD, Jousse C, Marciniak SJ, Zhang Y, Novoa I, Scheuner D, Kaufman RJ, Ron D, Harding HP. Cytoprotection by pre-emptive conditional phosphorylation of translation initiation factor 2. EMBO J. 2004; 23:169–179. [PubMed: 14713949]

McEwen E, Kedersha N, Song B, Scheuner D, Gilks N, Han A, Chen JJ, Anderson P, Kaufman RJ. Heme-regulated inhibitor kinase-mediated phosphorylation of eukaryotic translation initiation factor 2 inhibits translation, induces stress granule formation, and mediates survival upon arsenite exposure. J Biol Chem. 2005; 280:16925–16933. [PubMed: 15684421]

Nargund AM, Pellegrino MW, Fiorese CJ, Baker BM, Haynes CM. Mitochondrial import efficiency of ATFS-1 regulates mitochondrial UPR activation. Science. 2012; 337:587–590. [PubMed: 22700657]

Novoa I, Zeng H, Harding HP, Ron D. Feedback inhibition of the unfolded protein response by GADD34-mediated dephosphorylation of eIF2alpha. J Cell Biol. 2001; 153:1011–1022. [PubMed: 11381086]

Nunnari J, Suomalainen A. Mitochondria: in sickness and in health. Cell. 2012; 148:1145–1159. [PubMed: 22424226]

Rainey RN, Glavin JD, Chen HW, French SW, Teitell MA, Koehler CM. A new function in translocation for the mitochondrial i-AAA protease Yme1: import of polynucleotide phosphorylase into the intermembrane space. Mol Cell Biol. 2006; 26:8488–8497. [PubMed: 16966379]

Rugarli EI, Langer T. Mitochondrial quality control: a matter of life and death for neurons. EMBO J. 2012; 31:1336–1349. [PubMed: 22354038]

Runkel ED, Liu S, Baumeister R, Schulze E. Surveillance-activated defenses block the ROS-induced mitochondrial unfolded protein response. PLoS Genet. 2013; 9:e1003346. [PubMed: 23516373]

Ryan MT, Hoogenraad NJ. Mitochondrial-nuclear communications. Annu Rev Biochem. 2007; 76:701–722. [PubMed: 17227225]

Scheuner D, Song B, McEwen E, Liu C, Laybutt R, Gillespie P, Saunders T, Bonner-Weir S, Kaufman RJ. Translational control is required for the unfolded protein response and in vivo glucose homeostasis. Mol Cell. 2001; 7:1165–1176. [PubMed: 11430820]

Schmidt O, Harbauer AB, Rao S, Eyrich B, Zahedi RP, Stojanovski D, Schonfisch B, Guiard B, Sickmann A, Pfanner N, et al. Regulation of mitochondrial protein import by cytosolic kinases. Cell. 2011; 144:227–239. [PubMed: 21215441]

Schmidt O, Pfanner N, Meisinger C. Mitochondrial protein import: from proteomics to functional mechanisms. Nat Rev Mol Cell Biol. 2010; 11:655–667. [PubMed: 20729931]

Schroder M, Kaufman RJ. The mammalian unfolded protein response. Annu Rev Biochem. 2005; 74:739–789. [PubMed: 15952902]

Shoulders MD, Ryno LM, Genereux JC, Moresco JJ, Tu PG, Wu C, Yates JR 3rd, Su AI, Kelly JW, Wiseman RL. Stress-independent activation of XBP1s and/or ATF6 reveals three functionally diverse ER proteostasis environments. Cell Rep. 2013; 3:1279–1292. [PubMed: 23583182]

Sonenberg N, Hinnebusch AG. Regulation of translation initiation in eukaryotes: mechanisms and biological targets. Cell. 2009; 136:731–745. [PubMed: 19239892]

Tatsuta T. Protein quality control in mitochondria. J Biochem. 2009; 146:455–461. [PubMed: 19666648]

Vattem KM, Wek RC. Reinitiation involving upstream ORFs regulates ATF4 mRNA translation in mammalian cells. Proc Natl Acad Sci U S A. 2004; 101:11269–11274. [PubMed: 15277680]

Washburn MP, Wolters D, Yates JR 3rd. Large-scale analysis of the yeast proteome by multidimensional protein identification technology. Nat Biotechnol. 2001; 19:242–247. [PubMed: 11231557]

Wek RC, Cavener DR. Translational control and the unfolded protein response. Antioxid Redox Signal. 2007; 9:2357–2371. [PubMed: 17760508]

Wek RC, Jiang HY, Anthony TG. Coping with stress: eIF2 kinases and translational control. Biochem Soc Trans. 2006; 34:7–11. [PubMed: 16246168]

Wu S, Tan M, Hu Y, Wang JL, Scheuner D, Kaufman RJ. Ultraviolet light activates NFkappaB through translational inhibition of IkappaBalpha synthesis. J Biol Chem. 2004; 279:34898–34902. [PubMed: 15184376]

Yamasaki S, Anderson P. Reprogramming mRNA translation during stress. Curr Opin Cell Biol. 2008; 20:222–226. [PubMed: 18356035]

Yates JR, Ruse CI, Nakorchevsky A. Proteomics by mass spectrometry: approaches, advances, and applications. Annu Rev Biomed Eng. 2009; 11:49–79. [PubMed: 19400705]

Zhao Q, Wang J, Levichkin IV, Stasinopoulos S, Ryan MT, Hoogenraad NJ. A mitochondrial specific stress response in mammalian cells. EMBO J. 2002; 21:4411–4419. [PubMed: 12198143]

HIGHLIGHTS

- Tim17A is a stress-sensitive subunit of the TIM23 protein import complex

- Tim17A protein decrease in response to stress-regulated translation attenuation

- Tim17A degradation requires the activity of the mitochondrial protease YME1L

- Decreased Tim17A/Tim-17 is protective against oxidative stress
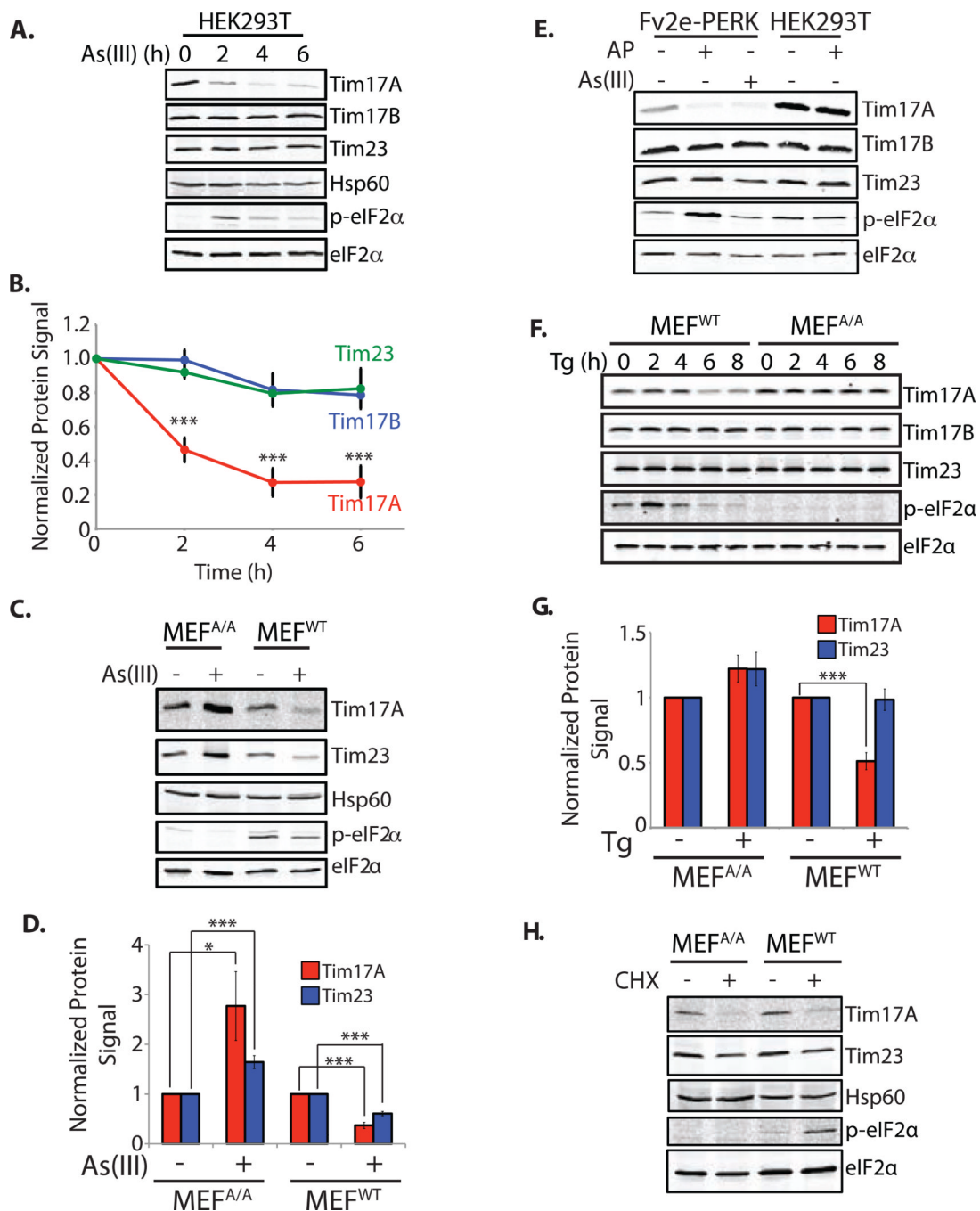
Figure 1. Tim17A Protein Levels are Reduced By Activation of the Integrated Stress Response (ISR)

A. Representative immunoblot of lysates prepared from HEK293T cells treated with As(III) (50 μM) for the indicated time.

B. Quantification of Tim17A, Tim17B, and Tim23 in immunoblots as shown in Figure 1A. Error bars represent SEM for n=5.

C. Representative immunoblot of lysates prepared from MEF^WT and MEF^A/A cells treated with As(III) (100 μM) for 8 h.

D. Quantification of Tim17A and Tim23 in immunoblots as shown in Figure 1C. Error bars indicate SEM for n=3.

E. Immunoblot of lysates prepared from HEK293 cells stably expressing Fv2e-PERK treated with AP20187 (5 nM) or As(III) (50 μM) for 6 h. HEK293T cells treated with AP20187 are shown as a control.

F. Immunoblot of MEF^{WT} and MEF$^{A/A}$ cells treated with thapsigargin (1 μM) for the indicated time.

G. Quantification of Tim17A and Tim23 at 6 h for immunoblots as shown in Figure 1F. Error bars indicate SEM for n=7.

H. Immunoblot of lysates prepared from MEF^{WT} and MEF$^{A/A}$ cells treated with cycloheximide (CHX; 50 μg/mL) for 6 h.

*indicates p-value<0.05, **indicates p-value<0.01, ***indicates p-value<.005.

see also Figure S1
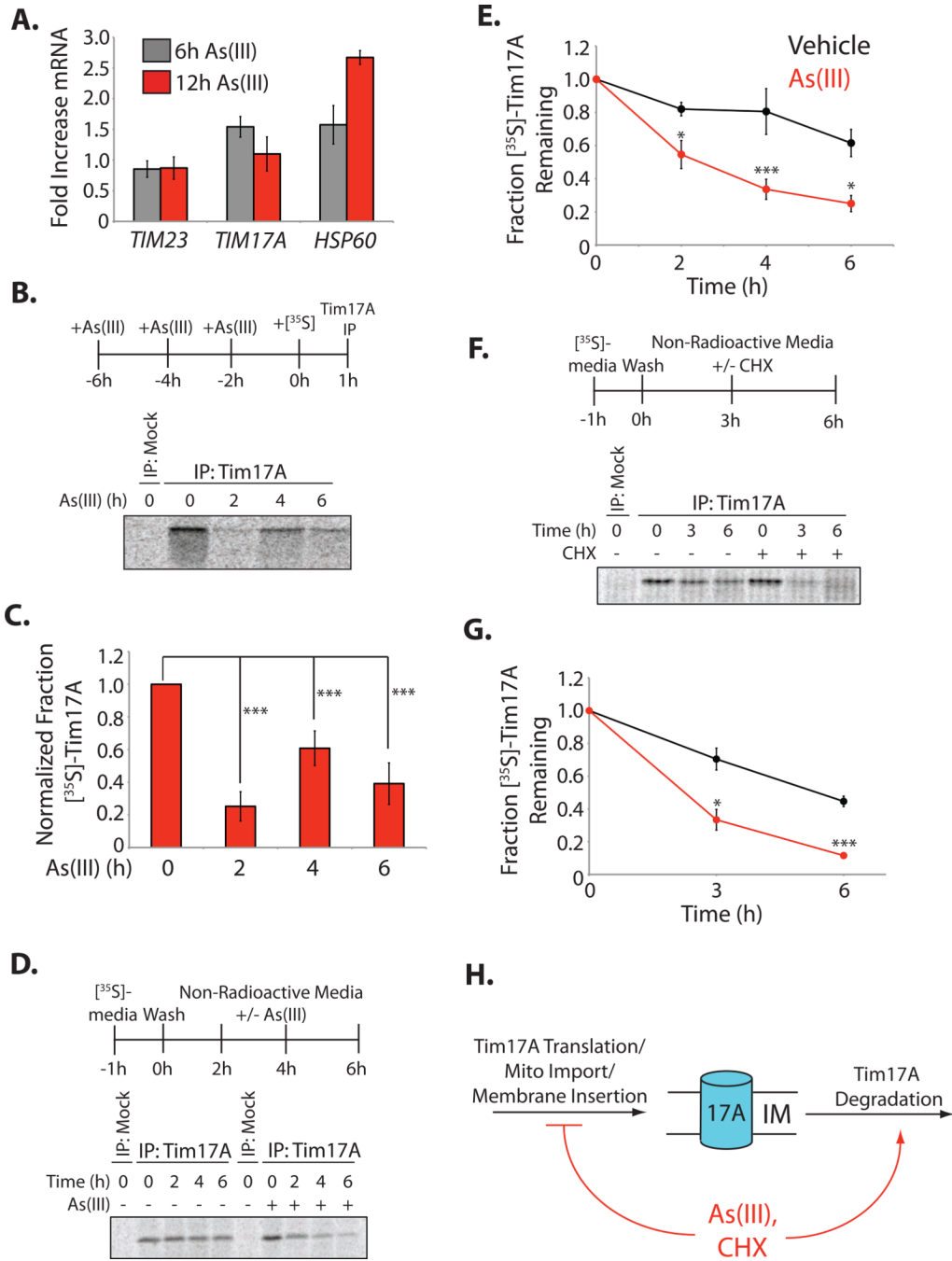
Figure 2. As(III) Reduces Tim17A Biogenesis and Increases Tim17A Targeting to Proteolytic Degradation

A. qPCR of *TIM23*, *TIM17A* and *HSP60* in HEK293T cells treated with As(III) (50 μM) for 6 h (grey) or 12 h (red). The error bars show the mean +/− 95% confidence interval.

B. Representative autoradiogram of newly-synthesized, [^{35}S]-labeled Tim17A immunopurified from HEK293T cells pretreated with As(III) (100 μM) for the indicated time. The labeling protocol is shown above.

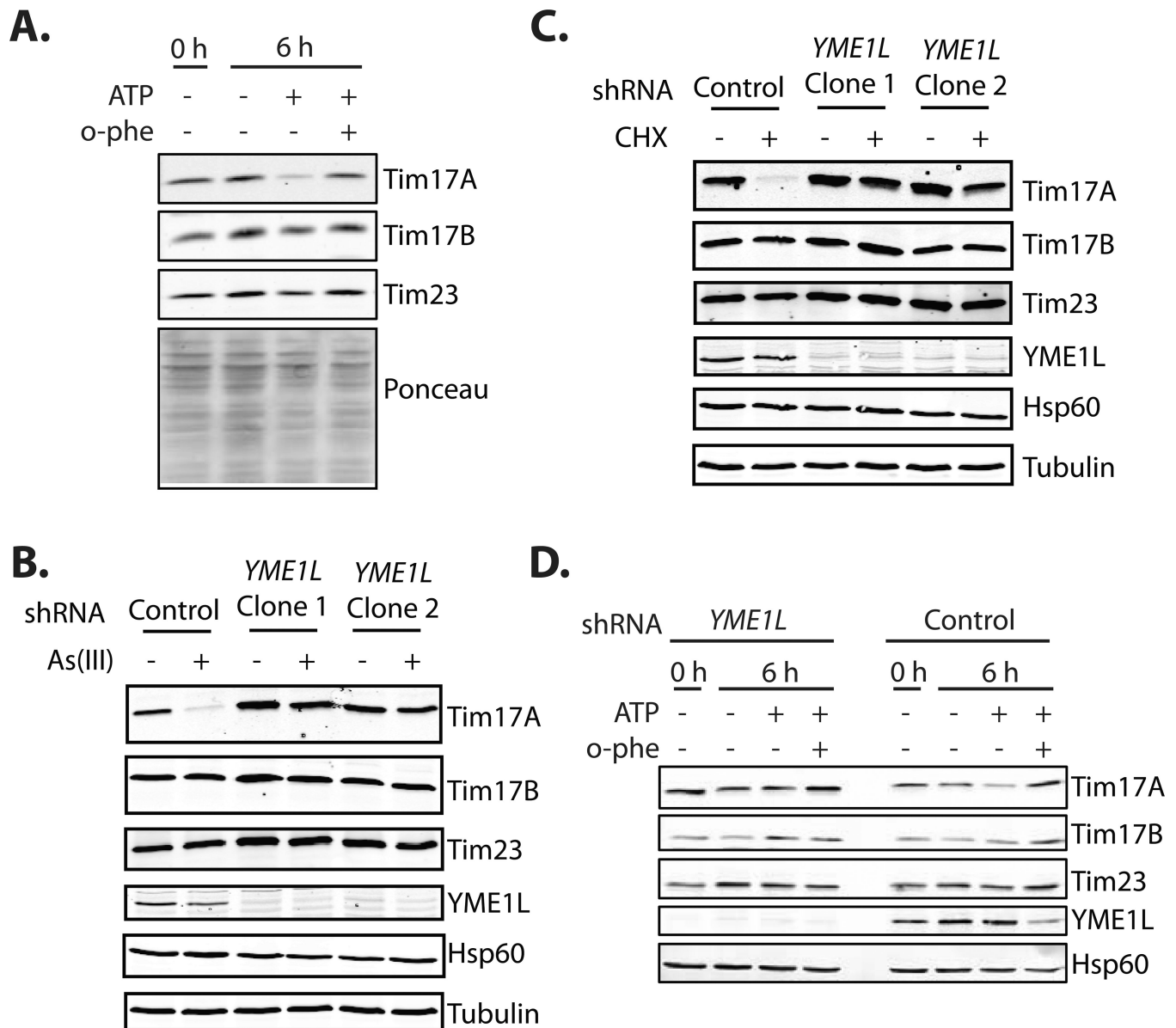**C**. Quantification of autoradiograms as shown in Figure 2B. Error bars represent SEM for n=4.

D. Representative autoradiogram of Tim17A immunopurified from HEK293T cells labeled with [^{35}S] then chased in the absence or presence of As(III) (100 μM) for the indicated time. The labeling protocol is shown above.

E. Quantification of autoradiograms as shown in Figure 2D. Error bars represent SEM from n 4.

F. Representative autoradiogram of Tim17A immunopurified from HEK293T cells labeled with [^{35}S] and chased in the absence or presence of cycloheximide (CHX; 50 μg/mL). The labeling protocol is shown above.

G. Quantification of autoradiograms as shown in Figure 2F. Error bars represent SEM from n 3.

H. Illustration showing that stress-dependent reductions in Tim17A results from both a decrease in Tim17A biogenesis and an increase in Tim17A targeting to proteolytic degradation.

*indicates p-value<0.05, **indicates p-value<0.01, ***indicates p-value<0.005.

see also Figure S2

A.

ATP − − + +
o-phe − − − +

0 h | 6 h

Tim17A
Tim17B
Tim23
Ponceau

C.

shRNA Control | YME1L Clone 1 | YME1L Clone 2
CHX − + − + − +

Tim17A
Tim17B
Tim23
YME1L
Hsp60
Tubulin

B.

shRNA Control | YME1L Clone 1 | YME1L Clone 2
As(III) − + − + − +

Tim17A
Tim17B
Tim23
YME1L
Hsp60
Tubulin

D.

shRNA YME1L | Control
0 h | 6 h | 0 h | 6 h
ATP − − + + − − + +
o-phe − − − + − − − +

Tim17A
Tim17B
Tim23
YME1L
Hsp60

Figure 3. Tim17A Degradation Requires the i-AAA Mitochondrial Protease YME1L
A. Immunoblot of extracts prepared from mitochondria isolated from HEK293T. Isolated mitochondria were treated with ATP (5 mM) and o-phenanthroline (o-phe; 1 mM) for 0 or 6 h at 37°C, as indicated.
B. Immunoblot of lysates prepared from SHSY5Y cells stably-expressing control or *YME1L* shRNA and treated with As(III) (50 μM; 6h), as indicated. Two separate stable lines expressing *YME1L* shRNA are shown.
C. Immunoblot of lysates prepared from SHSY5Y cells stably-expressing control or *YME1L* shRNA and treated with cycloheximide (CHX; 50 μg/mL; 6h), as indicated. Two separate stable lines expressing *YME1L* shRNA are shown.
D. Immunoblot of purified mitochondria isolated from HEK293T cells expressing control or *YME1L* shRNA. Mitochondria were incubated for 0 or 6 h at 37°C in the presence of ATP (5 mM) and o-phenanthroline (o-phe; 1mM), as indicated.
See also Figure S3
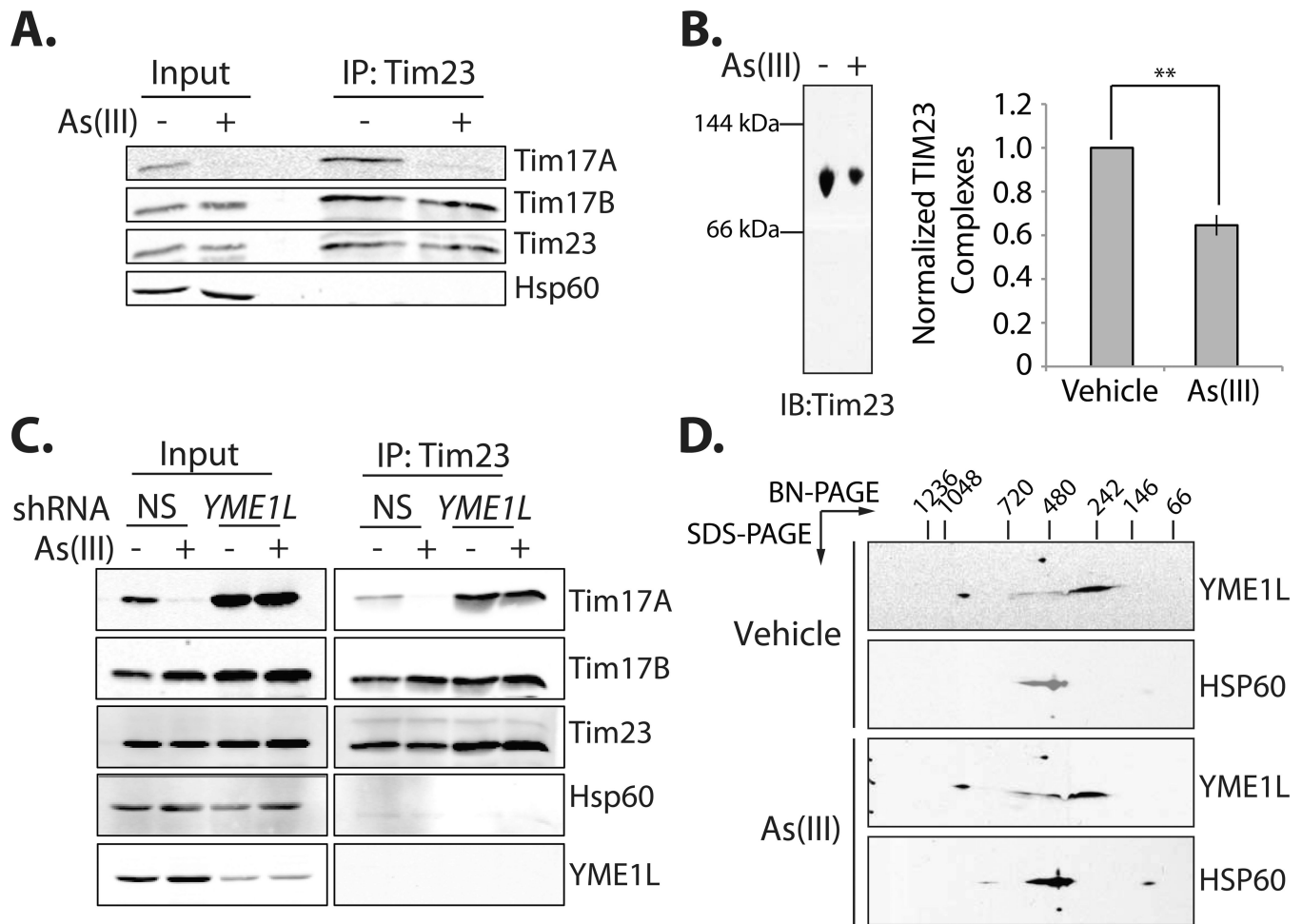
Figure 4. As(III) Does Not Induce Tim17A Dissociation from the TIM23 Complex
A. Immunoblot of Tim23 immunopurified from mitochondria isolated from SHSY5Y treated with or without As(III) (50 μM; 6 h).
B. BN-PAGE immunoblot and quantification of Tim23 in mitochondria isolated from HEK293Ttreated with As(III) (50 μM; 6 h), as indicated. Error bars represent SEM from n=3 experiments. **indicates p-value <0.01.
C. Immunoblot of Tim23 immunopurified from mitochondria isolated from HEK293T cells expressing control or *YME1L* shRNA treated with or without As(III) (50 μM; 6 h).
D. Immunoblot of BN-PAGE/SDS-PAGE of YME1L in mitochondria isolated from HEK293T cells treated with As(III) (50 μM; 6 h), as indicated. HSP60 oligomers are shown as a control.
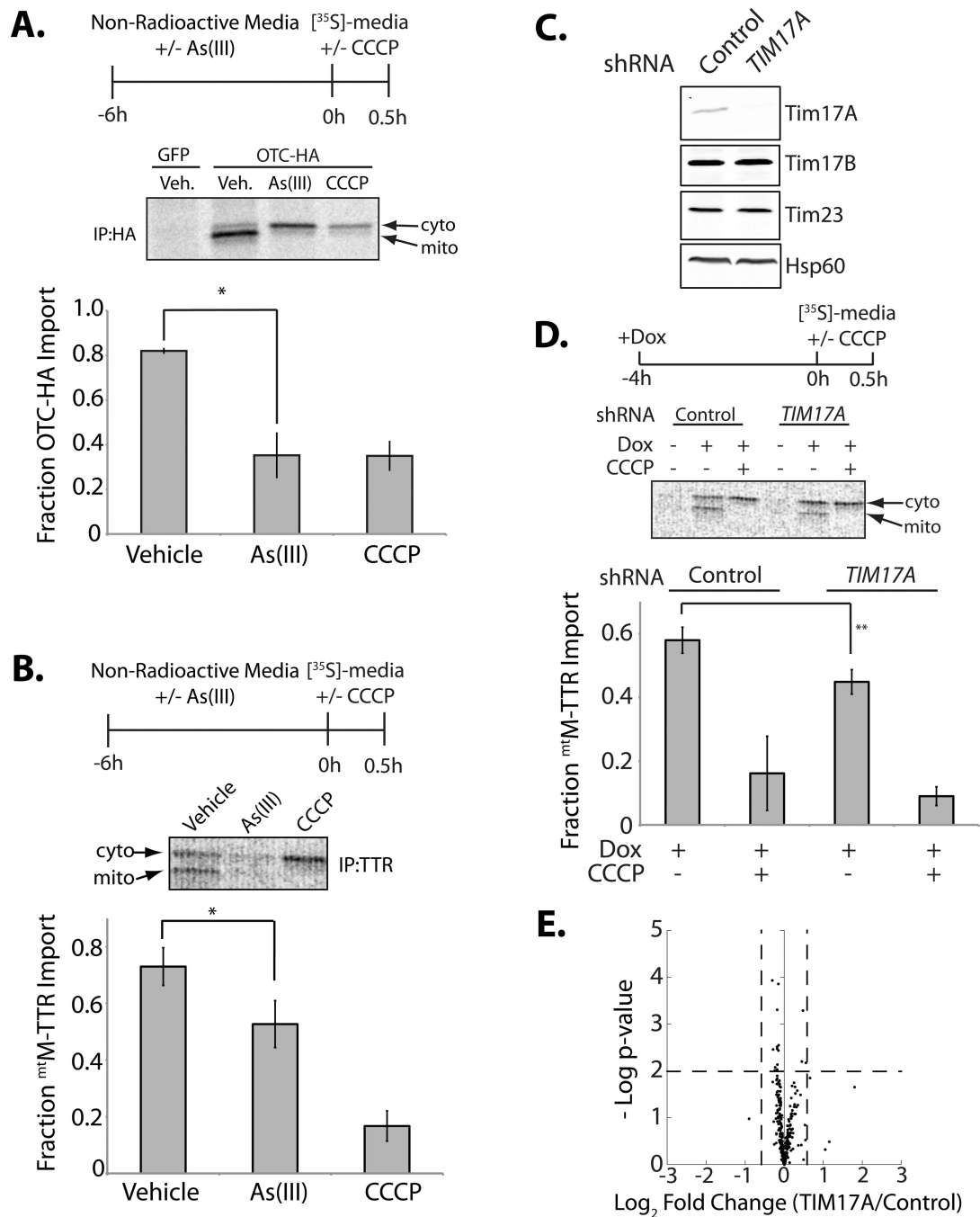
Figure 5. Reduced Tim17A Decreases TIM23 Mitochondrial Protein Import Efficiency
A. Representative autoradiogram and quantification of [^{35}S]-labeled OTC^{HA} in HEK293T cells pre-treated with As(III) (50 μM, 6 h), as indicated. Arrows show the cytosolic (cyto) and mitochondrial (mito) OTC^{HA}. The mitochondrial uncoupler CCCP (50 μM) was added coincident with [^{35}S]-Met/Cys, as indicated. The experimental paradigm is shown above. Fraction OTC^{HA} import was calculated as described in Experimental Procedures. Error bars show SEM from n=3.
B. Representative autoradiogram and quantification of [^{35}S]-labeled ^{mt}M-TTR in HEK293T cells pre-treated with As(III) (50 μM, 6 h), as indicated. Arrows indicate the cytosolic (cyto)

and mitochondrial (mito) ^{mt}M-TTR bands. The mitochondrial uncoupler CCCP (50 μM) was added coincident with [^{35}S]-Met/Cys, as indicated. The experimental paradigm is shown above. Fraction ^{mt}M-TTR import was calculated as described in Experimental Procedures. Error bars show SEM from n=5

C. Immunoblot of lysates prepared from HEK293T-Rex cells expressing control non-silencing shRNA or *TIM17A* shRNA.

D. Representative autoradiogram and quantification of cytosolic and mitochondrial ^{mt}M-TTR in HEK293TRex cells stably expressing control or *TIM17A* shRNA. Dox (1 μg/mL) was added for 4 h prior to labeling to induce tet-inducible ^{mt}M-TTR expression. CCCP (50 μM) was added during the label to the indicated cells. The experimental protocol is shown above the autoradiogram. Fraction ^{mt}M-TTR import was calculated as described in Experimental Procedures. Error bars show SEM from n=6.

E. Plot showing relative mitochondrial protein concentrations in HEK293T cells expressing control or *TIM17A* shRNA. The plot depicts the –log p-value vs. the $\log_2$ fold-change of protein concentration in *TIM17A*-depleted cells relative to cells expressing control shRNA. The 317 GO annotated mitochondrial proteins are shown. The vertical dashed lines represent fold changes >1.5 fold. The horizontal dashed line indicates a p-value < 0.01.

*indicates p-value<0.05, **indicates p-value<0.01.

see also Figure S4 and Table S1
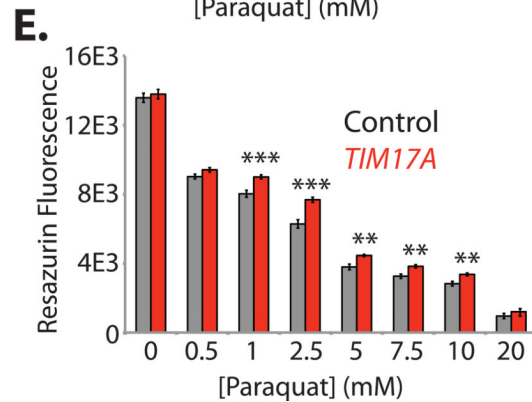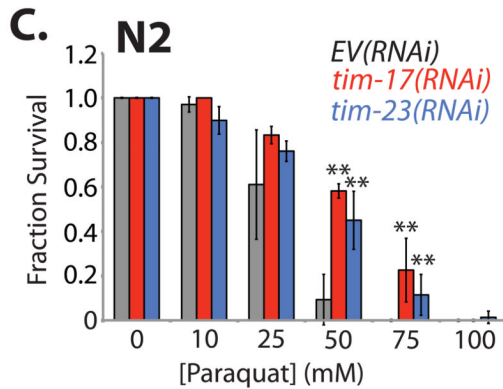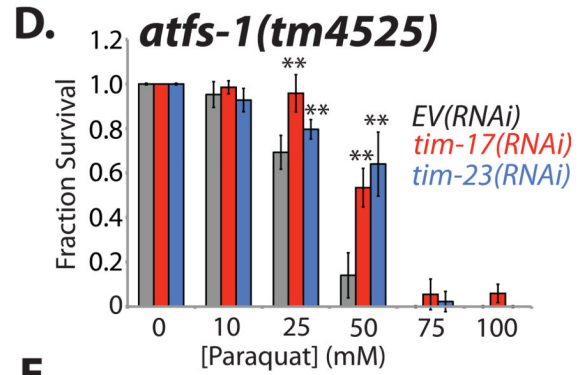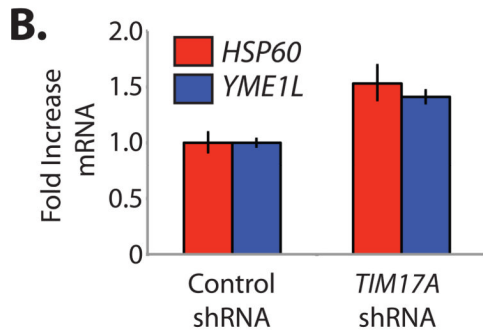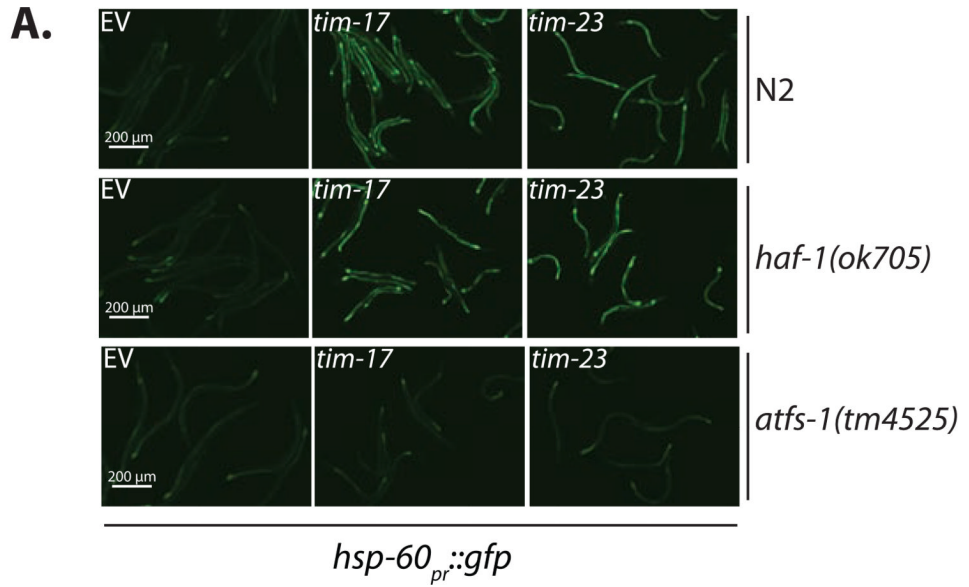
Figure 6. Decreasing Tim17A/TIM-17 Increases Expression of Stress-Responsive Mitochondrial Proteostasis Genes and Confers Stress-Resistance in *C. elegans* and Mammalian Cells
A. Representative images depicting the activation of the UPR^mt reporter *hsp-60_pr_::gfp* in *C. elegans* strains fed *E. coli* expressing empty vector (EV), *tim-17(RNAi)* or *tim-23(RNAi)*, as indicated. The strains used in this figure are N2 (wild-type; top), *haf-1(ok705)* (middle), and *atfs-1(tm4525)* (bottom).
B. qPCR of *HSP60* and *YME1L* in HEK293T cells stably-expressing control or *TIM17A* shRNA. mRNA levels were normalized to *GAPDH*. The error bars show the mean +/− 95% confidence interval. Data are representative of 3 independent experiments.

C. Survival analysis of N2 worms fed *E. coli* expressing empty vector (EV; black), *tim-17(RNAi)* (red) or *tim-23(RNAi)* (blue). Animals were treated with the indicated concentration of paraquat at Day 1 of adulthood. Animal survival was scored following a 24 h paraquat treatment. Error bars show SEM for n=8. Data are representative of 4 independent experiments.

D. Survival analysis of *atfs-1(tm4525)* mutant worms fed *E. coli* expressing empty vector (EV; black), *tim- 17(RNAi)* (red) or *tim-23(RNAi)* (blue). Animals were treated with the indicated concentration of paraquat at Day 1 of adulthood. Animal survival was scored following a 24 h paraquat treatment. Error bars show SEM for n=8. Data are representative of 4 independent experiments.

E. Bar graph showing the resazurin fluorescence of HEK293T cells expressing control or *TIM17A* shRNA and treated with the indicated concentration of paraquat for 24h. Error bars show SEM for n=8. Data are representative of 3 independent experiments.

**indicates p-value < 0.01, ***indicates p-value < 0.005.

see also Figure S5
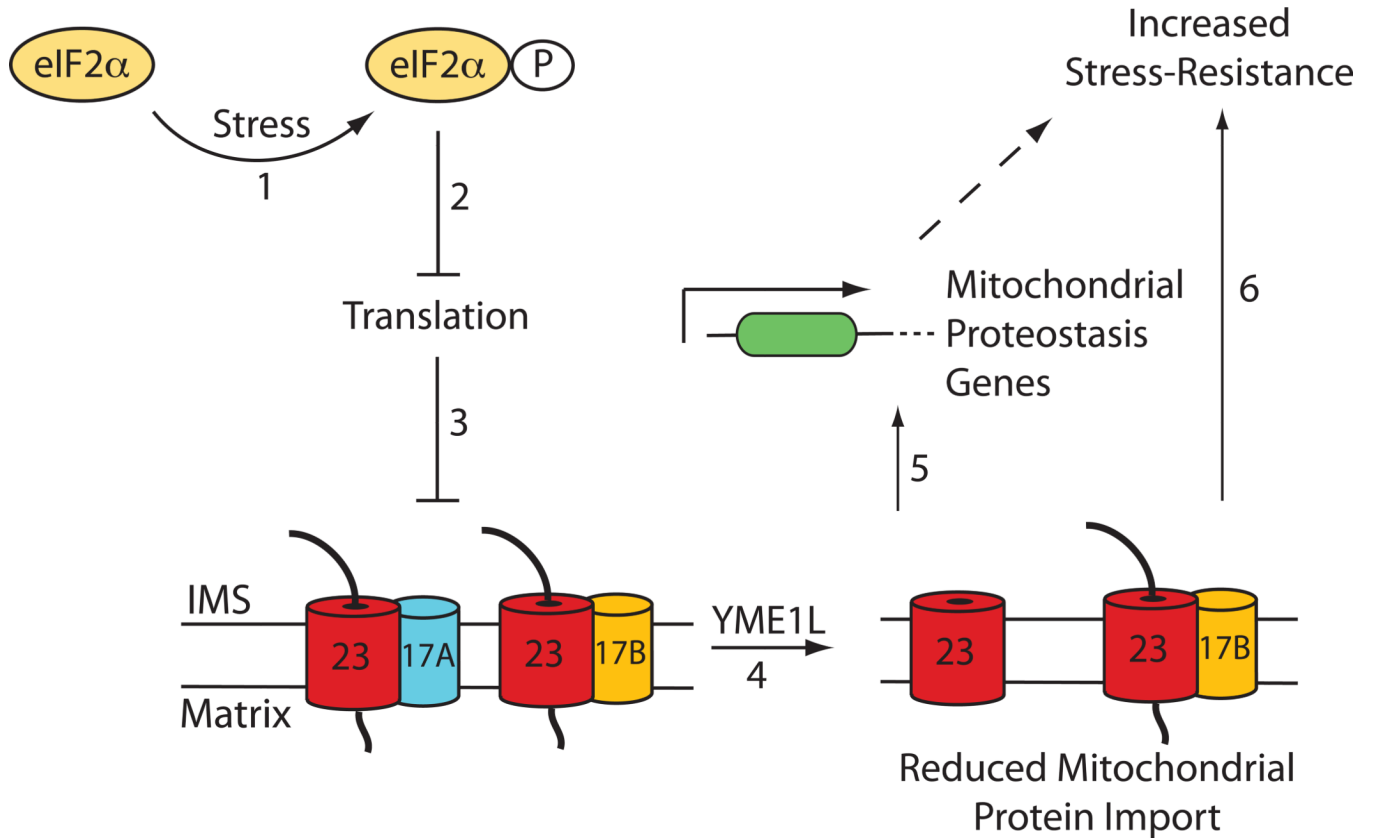
Figure 7. Model Showing the Predicted Mechanism of ISR-dependent Remodeling of Mitochondrial Protein Import Through Stress-Induced Tim17A Degradation
Pathologic insults (e.g. As(III), ER stress, etc) induce eIF2α phosphorylation (step 1), which leads to stress-regulated translational attenuation (step 2). Reduced translation decreases the stability of Tim17A protein levels through reduced Tim17A biogenesis (step 3) and increased YME1L-dependent Tim17A degradation (step 4). This decreases the population of active TIM23 complexes containing a core Tim23-Tim17A interaction, reducing TIM23 import efficiency and facilitating induction of stress-responsive mitochondrial proteostasis genes (step 5). Reduced TIM23 import activity also confers stress resistance through a mechanism independent of ATFS-1 mediated transcriptional upregulation of mitochondrial proteostasis genes (step 6).